Preparation, Properties, and Bonding Analysis of Tantalum(II) η^6-Arene Complexes

Pamela A. Wexler and David E. Wigley*

Department of Chemistry, University of Arizona, Tucson, Arizona 85721

John B. Koerner and Thomas A. Albright*

Department of Chemistry, University of Houston, Houston, Texas 77204-5641

Received October 9, 1990

The tantalum(III) η^6-arene complexes (η^6-C_6R_6)Ta(DIPP)$_2$Cl (DIPP = 2,6-diisopropyl phenoxide) undergo facile one-electron reductions to afford the paramagnetic Ta(II) arenes (η^6-C_6R_6)Ta(DIPP)$_2$. Thus, (η^6-C_6Et_6)Ta(DIPP)$_2$Cl (**1**), itself prepared by the cyclotrimerization of EtC≡CEt, reacts with excess NaHg to afford the maroon Ta(II) complex (η^6-C_6Et_6)Ta(DIPP)$_2$ (**3**) in high yield. Alternatively, **3** is prepared from the three-electron reduction of Ta(DIPP)$_2$Cl$_3$(OEt$_2$) in the presence of EtC≡CEt. Similarly, (η^6-C_6Me_6)Ta(DIPP)$_2$ (**4**) is prepared upon reducing (η^6-C_6Me_6)Ta(DIPP)$_2$Cl (**2**) with excess NaHg. (η^6-C_6Et_6)Ta(DIPP)$_2$ (**3**) undergoes one-electron oxidative addition reactions with CH_2Cl_2 to regenerate **1**, with allyl bromide to afford (η^6-C_6Et_6)Ta(DIPP)$_2$Br (**5**), and with CH_3CH_2I to provide (η^6-C_6Et_6)Ta(DIPP)$_2$I (**7**). (η^6-C_6Et_6)Ta(DIPP)$_2$ (**3**) crystallizes in the monoclinic space group $P2_1/c$, with a = 12.396 (4) Å, b = 17.344 (6) Å, c = 18.622 (4) Å, and β = 99.11 (2)°, with V = 3953.3 Å^3 and Z = 4 for a calculated density of 1.31 g cm^{-3}. The η^6-arene ligand in **3** is characterized by a folded or boatlike distortion, with two carbons making a close approach to the metal. The arene also displays a C_2, "twist-boat" deformation of the other four arene carbons. Molecular orbital calculations at the extended Hückel and ab initio level on (η^6-C_6H_6)Ta(OH)$_2$ are used to investigate the bonding and geometric distortions for these molecules. It is found that the boatlike deformation of the benzene ligand is primarily due to maximization of the overlap between an s hybridized $x^2 - y^2$ orbital at the metal and π^* on benzene. The peculiar C_2 deformation of the remaining four carbon atoms in the benzene ligand is tied to rotation of the ML$_2$ unit about the metal–benzene axis. At the ab initio level, a fully optimized structure was found to lie 19.8 kcal/mol lower in energy than one where the benzene ligand was constrained to be planar.

Introduction

Arene complexes of the transition metals[1] have proven essential to the understanding of aromatic C–H bond activation,[2] arene hydrogenation[3] and exchange reactions,[4] and alkyne cyclotrimerization chemistry.[5] Well-categorized examples of (η^6-arene)ML$_2$ complexes[1b] are typically restricted to late-transition-metal, 18-electron species, as exemplified by [(η^6-arene)RhL$_2$]$^+$,[6] (η^6-arene)RuL$_2$,[7] (η^6-arene)FeL$_2$,[8] and (η^6-arene)NiR$_2$.[9] While "electron deficient" arenes are well-known, particularly in the early metals,[10] the only electron-deficient (η^6-arene)ML$_2$ species seem to be the 17-electron (η^6-arene)CoR$_2$ derivatives.[11]

We have recently prepared tantalum(III) arenes of the form (η^6-C_6R_6)Ta(OR)$_2$Cl[12] and have discovered that they undergo a facile one-electron reduction to afford the paramagnetic tantalum(II) complexes (η^6-C_6R_6)Ta(OR)$_2$.[13] Since the electron count at the metal center is a nominal 13 electrons, these molecules represent extremely electron deficient (η^6-arene)ML$_2$-type complexes. Further interest in these species arises since the arene ligand was assembled at the metal center by alkyne cyclization chemistry[5,14] and since they represent rare examples of tantalum(II) or-

(1) (a) Silverthorn, W. E. *Adv. Organomet. Chem.* **1975**, *13*, 47. (b) Muetterties, E. L.; Bleeke, J. R.; Wucherer, E. J.; Albright, T. A. *Chem. Rev.* **1982**, *82*, 499.

(2) (a) Jones, W. D.; Feher, F. J. *J. Am. Chem. Soc.* **1984**, *106*, 1650. (b) Jones, W. D.; Feher, F. J. *Ibid.* **1982**, *104*, 4240.

(3) (a) Bleeke, J. R.; Muetterties, E. L. *J. Am. Chem. Soc.* **1981**, *103*, 556. (b) Muetterties, E. L.; Bleeke, J. R. *Acc. Chem. Res.* **1979**, *12*, 324 and references therein. (c) Steffey, B. D.; Chesnut, R. W.; Kerschner, J. L.; Pellechia, P. J.; Fanwick, P. E.; Rothwell, I. P. *J. Am. Chem. Soc.* **1989**, *111*, 378.

(4) (a) Muetterties, E. L.; Bleeke, J. R.; Sievert, A. C. *J. Organomet. Chem.* **1979**, *178*, 197. (b) Sievert, A. C.; Muetterties, E. L. *Inorg. Chem.* **1981**, *20*, 489.

(5) (a) Vollhardt, K. P. C. *Angew. Chem., Int. Ed. Engl.* **1984**, *23*, 539. (b) Vollhardt, K. P. C. In *Strategies and Tactics in Organic Synthesis*; Lindberg, T., Ed.; Academic Press: Orlando, 1984; pp 299–324. (c) McAlister, D. R.; Bercaw, J. E.; Bergman, R. G. *J. Am. Chem. Soc.* **1977**, *99*, 1666 and references therein.

(6) [(η^6-Arene)RhL$_2$]$^+$: (a) Albano, P.; Aresta, M.; Manassero, M. *Inorg. Chem.* **1980**, *19*, 1069. (b) Townsend, J. M.; Blount, J. F. *Inorg. Chem.* **1981**, *20*, 269. (c) Thompson, M. R.; Day, C. S.; Day, V. W.; Mink, R. I.; Meutterties, E. L. *J. Am. Chem. Soc.* **1980**, *102*, 2979. (d) Schrock, R. R.; Osborn, J. A. *J. Am. Chem. Soc.* **1971**, *93*, 3089. (e) Green, M.; Kuc, T. A. *J. Chem. Soc., Dalton Trans.* **1972**, 832. (f) Nolte, M. J.; Gafner, G.; Haines, L. M. *J. Chem. Soc., Chem. Commun.* **1969**, 1406. (g) Nolte, M. J.; Gafner, G. *Acta Crystallogr., Sect. B* **1974**, *B30*, 738.

(7) (η^6-Arene)RuL$_2$: (a) Bennett, M. A.; Matheson, T. W.; Robertson, G. B.; Smith, A. K.; Tucker, P. A. *Inorg. Chem.* **1980**, *19*, 1014. (b) Schmid, H.; Ziegler, M. L. *Chem. Ber.* **1976**, *109*, 132. (c) Huttner, G.; Lange, S.; Fischer, E. O. *Angew. Chem., Int. Ed. Engl.* **1971**, *10*, 556. (d) Huttner, G.; Lange, S. *Acta Crystallogr., Sect. B* **1972**, *B28*, 2049. (e) Werner, H.; Werner, R. *Angew. Chem., Int. Ed. Engl.* **1978**, *17*, 683.

(8) (η^6-Arene)FeL$_2$: (a) Green, M. L. H.; Wong, L. L. *J. Chem. Soc., Chem. Commun.* **1984**, 1442. (b) Radonovich, L. J.; Eyring, M. W.; Groshens, T. J.; Klabunde, K. J. *J. Am. Chem. Soc.* **1982**, *104*, 2816. (c) Weber, S. R.; Brintzinger, H. H. *J. Organomet. Chem.* **1977**, *127*, 45. (d) Ittel, S. D.; Tolman, C. A. *J. Organomet. Chem.* **1979**, *172*, C47.

(9) (η^6-Arene)NiR$_2$: (a) Radonovich, L. J.; Koch, F. J.; Albright, T. A. *Inorg. Chem.* **1980**, *19*, 3373. (b) Klabunde, K. J.; Anderson, B. B.; Bader, M.; Radonovich, L. J. *J. Am. Chem. Soc.* **1978**, *100*, 1313.

(10) See, for example: (a) Gardner, T. G.; Girolami, G. S. *Angew. Chem., Int. Ed. Engl.* **1988**, *27*, 1693. (b) Cloke, F. G. N.; Courtney, K. A. E.; Sameh, A. A.; Swain, A. C. *Polyhedron* **1989**, *8*, 1641. (c) King, R. B.; Braitsch, D. M.; Kapoor, P. N. *J. Am. Chem. Soc.* **1975**, *97*, 60. (d) Cloke, F. G. N.; Dix, A. N.; Green, J. C.; Perutz, R. N.; Seddon, E. A. *Organometallics* **1983**, *2*, 1150. (e) Solari, E.; Floriani, C.; Chiesi-Villa A.; Guastini, C. *J. Chem. Soc., Chem. Commun.* **1989**, 1747. (f) Cloke, F. G. N.; Green, M. L. H. *J. Chem. Soc., Dalton Trans.* **1981**, 1938.

(11) Radonovich, L. J.; Klabunde, K. J.; Behrens, C. B.; McCollor, D. P.; Anderson, B. B. *Inorg. Chem.* **1980**, *19*, 1221.

(12) (a) Bruck, M. A.; Copenhaver, A. S.; Wigley, D. E. *J. Am. Chem. Soc.* **1987**, *109*, 6525. (b) Ballard, K. R.; Gardiner, I. M.; Wigley, D. E. *Ibid.* **1989**, *111*, 2159.

(13) Wexler, P. A.; Wigley, D. E. *J. Chem. Soc., Chem. Commun.* **1989**, 664.

(14) Arney, D. J.; Wexler, P. A.; Wigley, D. E. *Organometallics* **1990**, *9*, 1282.

0276-7333/91/2310-2319$02.50/0

ganometallics.[15] The molecular structure of one of these species, $(\eta^6\text{-}C_6Et_6)Ta(DIPP)_2$ (where DIPP = 2,6-diisopropyl phenoxide) has been determined and is shown to exhibit some unusual structural properties; thus, molecular orbital calculations at the extended Hückel and ab initio level on $(\eta^6\text{-}C_6H_6)Ta(OH)_2$ are used to investigate the bonding and geometric distortions for these molecules. A portion of this work has been communicated.[13]

Experimental Section

General Synthetic Details. All syntheses were performed under a nitrogen atmosphere either by standard Schlenk techniques[16] or in a Vacuum Atmospheres HE-493 drybox at room temperature (unless otherwise indicated). Solvents were purified under N_2 by standard techniques[17] and transferred to the drybox without exposure to air. $Ta(DIPP)_2Cl_3(OEt_2)$[14] and $(\eta^6\text{-}C_6Me_6)Ta(DIPP)_2Cl$[12b] (2) (DIPP = 2,6-diisopropyl phenoxide) were prepared as described previously. Allyl bromide, 1,2-dibromoethane, and iodoethane were obtained from Aldrich, and 3-hexyne was purchased from Farchan Laboratories. These reagents were passed down a short (ca. 5–6 cm) column of activated alumina (at ca. −10 °C) prior to use. The "cold" solvents used to wash isolated solids were at ca. −30 °C.

Physical Measurements. ^1H (250 MHz) and ^{13}C (62.9 MHz) NMR spectra were recorded at probe temperature (unless otherwise specified) on a Bruker WM-250 spectrometer in C_6D_6 solvent. Chemical shifts are referenced to protio impurities (δ 7.15) or solvent ^{13}C resonances (δ 128.0) and are reported downfield of Me_4Si. Infrared spectra in the region 1600–180 cm^{-1} were recorded as CsI pellets on a Perkin-Elmer PE-983 spectrometer or from 4000 to 600 cm^{-1} as a Nujol mull (NaCl plates) on a Perkin-Elmer 1310 instrument and were not assigned. Molecular weight measurements were determined by vapor pressure osmometry, using a device similar to one previously described.[18] Cyclic voltammetry experiments were performed under a nitrogen atmosphere with a BioAnalytical Systems CV-27 voltammograph and recorded on a Houston Instruments Model 100 X-Y recorder. Measurements were taken at a Pt-disk electrode in THF solutions containing 0.1 M $n\text{-}Bu_4NPF_6$ as supporting electrolyte. Voltammograms were recorded at room temperature at a sweep rate of 150 mV/s. Potentials were referenced to Ag/AgCl and are uncorrected for junction potentials. Magnetic moment measurements were performed by the Evan's method[19] on C_6D_6 solutions (250 MHz) at probe temperature, and frequency shifts were measured for solvent protio impurity resonances. Diamagnetic corrections (χ_{dia}) were calculated from Pascal's constants.[20] X-Band ESR spectra were recorded on toluene solutions by using a Varian E-3 spectrometer. All microanalytical samples were handled under nitrogen and were combusted with WO_3 (Desert Analytics, Tucson, AZ).

Preparations. $(\eta^6\text{-}C_6Et_6)Ta(DIPP)_2Cl$ **(1).** A solution of 2.00 g (2.79 mmol) of $Ta(DIPP)_2Cl_3(OEt_2)$ in 50 mL of diethyl ether was prepared and cooled to −40 °C. To this stirred solution were added 1.00 mL (8.80 mmol) of 3-hexyne and 2.00 mL (5.60 mmol) of a 0.47% NaHg amalgam. After being stirred at room temperature for 1 h, the resulting blue solution was filtered through Celite (Et_2O wash) and the solvent was removed from the filtrate in vacuo. The resulting blue solid was washed with 5–10 mL of cold pentane, filtered off, and dried in vacuo to provide 1.22 g (1.49 mmol, 53% yield) of product. This compound was recrystallized from toluene/pentane solutions to afford analytically pure samples. ^1H NMR (C_6D_6): δ 7.11–6.93 (A_2B m, 6 H, H_{aryl}), 3.23 (spt, 4 H, $CHMe_2$), 2.37 (q, 12 H, CH_2CH_3), 1.19 (d, 24 H, $CHMe_2$), 1.09 (t, 12 H, CH_2CH_3). ^{13}C NMR (C_6D_6): δ 156.1 (C_{ipso}), 137.1 (C_o), 126.8 (C_6Et_6), 123.6 (C_m), 122.4 (C_p), 25.7 ($CHMe_2$), 25.1 ($CHMe_2$), 23.9 (CH_2CH_3), 17.7 (CH_2CH_3). IR (Nujol): 1580 (w), 1435 (s), 1320 (m), 1254 (s), 1193 (sh), 1182 (s), 1098 (m), 1091 (m), 1038 (m), 930 (w), 904 (s), 885 (w), 861 (m), 820 (w), 788 (m), 742 (s), 700 cm^{-1} (m). Anal. Calcd for $C_{42}H_{64}ClO_2Ta$: C, 61.72; H, 7.89. Found: C, 62.30; H, 8.21.

$(\eta^6\text{-}C_6Et_6)Ta(DIPP)_2$ **(3). (i) From** $(\eta^6\text{-}C_6Et_6)Ta(DIPP)_2Cl$**.** To a room-temperature solution of 1.00 g (1.22 mmol) of $(\eta^6\text{-}C_6Et_6)Ta(DIPP)_2Cl$ (1) in 20 mL of diethyl ether was added excess NaHg amalgam (0.80 mL, 2.44 mmol, of a 0.46% amalgam). After being stirred for 24 h, this mixture was filtered through Celite and the solvent removed from the filtrate in vacuo to afford a red solid. When this solid was dissolved in minimal pentane and the solution cooled to −40 °C, dark red cubes (0.63 g, 0.81 mmol, 66%) formed and were filtered off, washed with minimal cold pentane, and dried in vacuo. Samples of compound obtained in this fashion were analytically pure.

(ii) From $Ta(DIPP)_2Cl_3(OEt_2)$**.** To a −40 °C solution of 1.00 g (1.40 mmol) of $Ta(DIPP)_2Cl_3(OEt_2)$ in 25 mL of diethyl ether were added 0.50 mL (4.40 mmol) of 3-hexyne and 2.00 mL (5.60 mmol) of 0.50% NaHg amalgam. The reaction was allowed to stir for 24 h at room temperature. The resulting dark red solution was filtered through Celite, and the filtrate was pumped to dryness. The resulting dark red solid was dissolved in pentane and cooled to −40 °C. A 0.35-g (0.45 mmol, 32% yield) sample of maroon crystals was filtered off, washed with a minimal volume of cold pentane, and dried in vacuo. ^1H NMR (C_6D_6) [all resonances are broad, featureless signals (peak width at half-maximum (in Hz) in parentheses)]: δ 9.70 (40), 4.73 (135), 4.06 (80), 3.77 (90). IR (CsI): 1588 (m, w), 1453 (sh), 1434 (s), 1380 (m), 1359 (m), 1336 (s), 1326 (s), 1268 (s), 1258 (s), 1206 (s), 1104 (m), 1057 (m), 1044 (m), 904 (s), 875 (m), 823 (m), 791 (m), 748 (s), 707 (m, s), 593 (m, w), 419 (w), 258 cm^{-1} (w). Molecular weight (Et_2O solution): calcd. for monomer, 781.9; found, 809 ± 80. Magnetic moment (C_6D_6 solution): μ_{eff} = 2.14 μ_B. Anal. Calcd for $C_{42}H_{64}O_2Ta$: C, 64.52; H, 8.25; Cl, 0.00. Found: C, 65.01; H, 8.57; Cl, <0.05.

$(\eta^6\text{-}C_6Me_6)Ta(DIPP)_2$ **(4).** To a room-temperature solution of 1.19 g (1.62 mmol) of $(\eta^6\text{-}C_6Me_6)Ta(DIPP)_2Cl$ (2) in 20 mL of diethyl ether was added 0.70 mL (3.24 mmol) of a 0.50% NaHg amalgam. This mixture was stirred for 24 h, over which time a gradual color change from blue to deep red was observed. The solution was then filtered through Celite, and the filtrate was pumped to dryness. The resulting red solid was dissolved in ca. 10 mL of pentane, and upon cooling to −40 °C, 0.37 g (0.53 mmol, 32% yield) of red brown plates were obtained. The product was collected, washed with minimal cold pentane, and dried in vacuo. This product was analytically pure. ^1H NMR (C_6D_6) [all resonances are broad, featureless signals (peak width at half-maximum (in Hz) in parentheses)]: δ 9.68 (30), 6.14 (20), 4.27 (65). IR (Nujol): 1580 (w), 1430 (s), 1328 (s), 1256 (s), 1200 (s), 1106 (m), 1088 (m), 1036 (m), 929 (w), 895 (s), 870 (m), 786 (m), 743 (s), 698 cm^{-1} (m). Magnetic moment (C_6D_6 solution): μ_{eff} = 2.07 μ_B. Anal. Calcd for $C_{36}H_{52}O_2Ta$: C, 61.97; H, 7.51. Found: C, 61.62; H, 7.63.

$(\eta^6\text{-}C_6Et_6)Ta(DIPP)_2Br$ **(5).** To a room-temperature solution of 0.25 g (0.32 mmol) of $(\eta^6\text{-}C_6Et_6)Ta(DIPP)_2$ (3) in 10 mL of diethyl ether was added 0.03 mL (0.32 mmol) of allyl bromide, whereupon the solution immediately turned blue. After being stirred for 5 min, the blue solution was pumped to dryness. The resulting blue solid was washed with 3–5 mL of cold pentane, filtered off, and dried in vacuo to provide 0.14 g (0.16 mmol, 50%) of product. Analytically pure compound was obtained upon recrystallizing the product from pentane at −40 °C. ^1H NMR (C_6D_6): δ 7.11–6.93 (A_2B m, 6 H, H_{aryl}), 3.21 (spt, 4 H, $CHMe_2$), 2.40 (q, 12 H, CH_2CH_3), 1.19 (d, 24 H, $CHMe_2$), 1.10 (t, 18 H, CH_2CH_3). ^{13}C NMR (C_6D_6): δ 156.6 (C_{ipso}), 137.0 (C_o), 126.7 (C_6Et_6), 123.6 (C_m), 122.4 (C_p), 25.8 ($CHMe_2$), 25.2 ($CHMe_2$), 24.3

(15) (a) Curtis has recently prepared tantalum(II) organometallic complexes of the form $[(\eta^5\text{-}C_5Me_5)Ta(CO)_2Cl]_2$ and $[(\eta^5\text{-}C_5Me_5)Ta(PhC{\equiv}CPh)Cl]_2$, similar to his previously reported niobium analogues. We thank Prof. M. D. Curtis (University of Michigan) for informing us of these results. For Curtis' niobium(II) complexes, see: Curtis, M. D.; Real, J. *Organometallics* **1985**, *4*, 940. (b) A compound of the apparent formulation $[TaBr_2(C_6Me_6)]_n$ has been reported (ref 10c) and the Ta(II) complex $[Ta_2Cl_4(C_6Me_6)]_2$ may have been isolated in an impure state, see: Fischer, E. O.; Röhrscheid, F. *J. Organomet. Chem.* **1966**, *6*, 53.

(16) Shriver, D. F.; Drezdzon, M. A. *The Manipulation of Air-Sensitive Compounds*, 2nd ed.; John Wiley and Sons: New York, 1986.

(17) Perrin, D. D.; Armarego, W. L. F. *Purification of Laboratory Chemicals*, 3rd ed.; Pergamon Press: Oxford, U.K. 1988.

(18) Burger, B. J.; Bercaw, J. E. In *Experimental Organometallic Chemistry*, Wayda, A. L., Darensbourg, M. Y., Eds.; ACS Symposium Series 357; American Chemical Society: Washington, DC, 1987.

(19) Evans, D. F. *J. Chem. Soc.* **1959**, 2003.

(20) Selwood, P. W. *Magnetochemistry*; Interscience Publishers, Inc.; New York, 1956.

(CH_2CH_3), 17.9 (CH_2CH_3). IR (Nujol): 1580 (w), 1430 (s), 1318 (m), 1250 (s), 1242 (sh), 1185 (sh), 1180 (s), 1096 (m), 1090 (m), 1048 (m, w), 902 (m, s), 885 (w), 859 (m), 784 (w), 741 (s), 697 cm^{-1} (w). Anal. Calcd for $C_{42}H_{64}BrO_2Ta$: C, 58.53; H, 7.48. Found: C, 58.45; H, 7.60.

(η^6-C_6Et_6)Ta(DIPP)Br_2 (6). To a solution of 0.25 g (0.32 mmol) of (η^6-C_6Et_6)Ta(DIPP)$_2$ (3) in 10 mL of diethyl ether was added 0.12 mL (1.40 mmol) of 1,2-dibromoethane, resulting in an immediate color change from red to blue. After being stirred for 15 min at room temperature, the solvent was removed in vacuo to provide a turquoise oil. The oil was reconstituted in room-temperature pentane, and within minutes, 0.05 g (0.07 mmol, 22% yield) of green crystals formed. The product was filtered off, leaving behind a blue filtrate, which was shown to contain (η^6-C_6Et_6)Ta(DIPP)$_2$Br (5). Samples of (η^6-C_6Et_6)Ta(DIPP)Br_2 (6) obtained in this fashion were always contaminated with varying amounts of (η^6-C_6Et_6)Ta(DIPP)$_2$Br (5), which could not be separated by fractional crystallization or chromatography; therefore no elemental analyses were attempted. ^1H NMR (C_6D_6): δ 7.06–6.90 (m, 3 H, H_{aryl}), 3.51 (spt, 2 H, $CHMe_2$), 2.09 (q, 12 H, CH_2CH_3), 1.32 (d, 12 H, $CHMe_2$), 0.93 (t, 18 H, CH_2CH_3).

(η^6-C_6Et_6)Ta(DIPP)$_2$I (7). To a room-temperature solution of 0.25 g (0.32 mmol) of (η^6-C_6Et_6)Ta(DIPP)$_2$ (3) in 10 mL of diethyl ether was added 0.03 mL (0.32 mmol) of iodoethane, whereupon the solution immediately turned purple. After being stirred for 5 min, the solvent was removed in vacuo and the resulting oil was reconstituted in 3 mL of pentane. Cooling this solution to −40 °C for 24 h afforded 0.13 g (0.14 mmol, 45%) of dark blue crystals. The crystals were collected, washed with minimal cold pentane, and dried in vacuo. Samples obtained in this fashion were analytically pure. ^1H NMR (C_6D_6): δ 7.11–6.92 (A_2B m, 6 H, H_{aryl}), 3.19 (spt, 4 H, $CHMe_2$), 2.42 (q, 12 H, CH_2CH_3), 1.20 (d, 24 H, $CHMe_2$), 1.11 (t, 18 H, CH_2CH_3). ^{13}C NMR (C_6D_6): δ 157.3 (C_{ipso}), 136.8 (C_o), 126.0 (C_6Et_6), 123.7 (C_m), 122.5 (C_p), 25.9 ($CHMe_2$), 25.4 ($CHMe_2$), 25.1 (CH_2CH_3), 18.1 (CH_2CH_3). IR (CsI): 1587 (w), 1536 (w), 1455 (sh), 1433 (s), 1381 (m), 1360 (m), 1323 (s), 1256 (s), 1195 (s), 1104 (s), 1045 (m), 909 (s), 892 (m), 866 (s), 827 (w), 792 (m), 747 (s), 706 (m), 624 (w), 601 (m), 590 (m), 429 (w), 343 (m), 314 (m, w), 301 (m, w), 259 cm^{-1} (w). Anal. Calcd for $C_{42}H_{64}IO_2Ta$: C, 55.51; H, 7.10. Found: C, 56.02; H, 7.43.

X-ray Structural Determination of (η^6-C_6Et_6)Ta(DIPP)$_2$. A maroon red, irregular crystal of (η^6-C_6Et_6)Ta(DIPP)$_2$ (3) grown from pentane solution and having approximate dimensions 0.35 × 0.45 × 0.40 mm was mounted in a glass capillary in a random orientation. Preliminary examination and data collection were performed at room temperature with Mo Kα radiation on a Syntex $P2_1$ diffractometer equipped with a graphite crystal incident beam monochromator. From the systematic absences of $h0l$, $l = 2n + 1$, and $0k0$, $k = 2n + 1$, and from the subsequent least-squares refinement, the space group was determined to be $P2_1/c$ (No. 14). As a check on crystal quality, three check reflections were measured after every 97 data reflections. The intensities of these standards remained constant within experimental error throughout data collection. A total of 7748 reflections were collected in the $+h,+k,\pm l$ octants (7008 unique) in the range $2° \le 2\theta \le 50°$, with 4581 reflections having $I > 3.0\sigma(I)$. The structure was solved by the Patterson method and refined by full-matrix least-squares techniques, for a final $R = 0.029$ and $R_w = 0.033$. Lorentz–polarization and empirical absorption corrections were applied. Hydrogen atoms were located and added to the structure factor calculations, but their positions were not refined. The highest peak in the final difference Fourier had a height of 1.03 e/Å^3. All calculations were performed on a VAX computer using SDP/VAX.[21]

Computational Details. The extended Hückel calculations[22] used a modified Wolfsberg–Helmholz formula[23] with the parameters listed in Table I taken from the literature.[24] The following bond lengths were used: C–H, 1.08 Å; C–C, 1.45 Å; Ta–O, 1.92 Å; O–H, 0.96 Å; Ta–benzene centroid, 1.91 Å for (η^6-C_6H_6)Ta(OH)$_2$. The C–C–C, C–C–H, and Ta–O–H angles were idealized at 120.0, 120.0, and 180.0°, respectively. The O–Ta–O angle was fixed at 96.1°. The ab initio UHF SCF calculations on (η^6-C_6H_6)Ta(OH)$_2$ utilized the GAUSSIAN 82 package.[25] A relativistic core potential was employed for the 1s to 5s electrons on Ta.[26] An associated double-ζ basis[26] was used for the valence region of the form (341/321/21). The standard 3-21G basis[27] was used for C, O, and H. All geometric parameters were fully optimized within a C_{2v} or C_2 symmetry constraint, as specified in the text. The values of $\langle s^2 \rangle$ ranged from 0.7767 to 0.7501 for the fully optimized geometries. Full listings of the internal coordinates and total energies are given in the supplementary material.

Table I. Parameters for the Extended Hückel Calculations

orbital	H_{ii}, eV	ξ_1	ξ_2	C_1[a]	C_2[a]
Ta 5d	-12.10	4.762	1.938	0.6815	0.5774
6s	-10.10	2.280			
6p	-6.86	2.241			
C 2s	-21.40	1.625			
2p	-11.40	1.625			
O 2s	-32.30	2.275			
2p	-14.80	2.275			
H 1s	-13.60	1.300			

[a] Coefficients used in the double-ζ expansion.

Results and Discussion

Synthesis and Reactivity of Tantalum(II) Arene Complexes. Ta(DIPP)$_2$Cl$_3$(OEt$_2$) (DIPP = 2,6-diisopropyl phenoxide) can be reduced by two electrons in the presence of RC≡CR (R = Me, Et) to afford the blue tantalum(III) arene complexes (η^6-C_6R_6)Ta(DIPP)$_2$Cl. The preparation of (η^6-C_6Me_6)Ta(DIPP)$_2$Cl (2) has been detailed,[12b] but optimum conditions for the synthesis of its hexaethylbenzene analogue (η^6-C_6Et_6)Ta(DIPP)$_2$Cl (1) are considerably different, and they are provided in the Experimental Section of this paper. As outlined in eq 1, both (η^6-

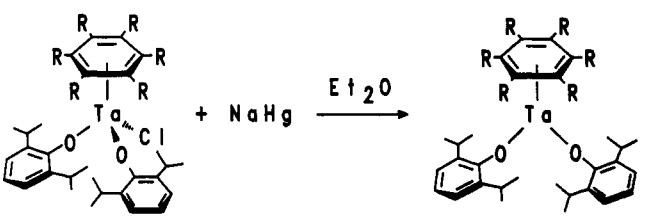

1, R = Et 3, R = Et
2, R = Me 4, R = Me

(1)

C_6R_6)Ta(DIPP)$_2$Cl compounds may be reduced further by one electron to provide the paramagnetic tantalum(II) monomers, (η^6-C_6R_6)Ta(DIPP)$_2$ (3, R = Et; 4, R = Me) in good yield. Thus, (η^6-C_6Et_6)Ta(DIPP)$_2$ (3) can be crystallized as maroon crystals in 66% yield from cold pentane solutions. Since this hexaethylbenzene compound is available in higher yields and is easier to isolate and purify than (η^6-C_6Me_6)Ta(DIPP)$_2$ (4), most of the reactivity studies (vide infra) were performed with 3 rather than 4. Alternatively, 3 can be prepared directly from Ta(DIPP)$_2$Cl$_3$(OEt$_2$) upon its reduction by three electrons in

(21) Frenz, B. A. In *Computing in Crystallography*; Schenk, H. R., Olthof-Hazelkamp, R., van Konigsfeld, H., Bassi, G. C., Eds.; Delft University Press: Delft, Holland, 1978; pp 64–71.
(22) (a) Hoffmann, R.; Lipscomb, W. N. *J. Chem. Phys.* **1962**, *36*, 2179, 3489; **1962**, *37*, 2782. (b) Hoffmann, R. *Ibid.* **1963**, *39*, 1397.
(23) Ammeter, J. H.; Bürgi, H.-B.; Thibeault, J. C.; Hoffmann, R. *J. Am. Chem. Soc.* **1978**, *100*, 3686.
(24) Hoffman, D. M.; Hoffmann, R.; Fisel, C. R. *J. Am. Chem. Soc.* **1982**, *104*, 3858.
(25) Binkley, J. S.; Frisch, M. J.; De Frees, D. J.; Raghavachari, K.; Whiteside, R. A.; Schlegel, H. B.; Pople, J. A. GAUSSIAN 82; Carnegie-Mellon Publishing Unit: Pittsburgh, 1984.
(26) Hay, P. J.; Wadt, W. R. *J. Chem. Phys.* **1985**, *82*, 299.
(27) Binkley, J. S.; Pople, J. A.; Hehre, W. J. *J. Am. Chem. Soc.* **1980**, *102*, 939.

the presence of EtC≡CEt, eq 2. The intermediate blue

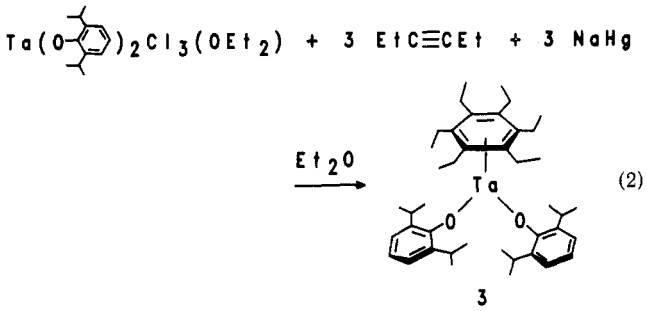

(2)

color in this reaction as well as the results of reaction 1 leaves little doubt as to the intermediacy of (η^6-C_6Et_6)-Ta(DIPP)$_2$Cl (1) in eq 2.

Magnetic moment measurements (Evans method[19]) on solutions of 3 and 4 yield values for μ_{eff} of around 2.1 μ_B for both compounds, which suggests the d^3 metal centers contain one unpaired electron with an orbital contribution to the moment. (η^6-C_6Et_6)Ta(DIPP)$_2$ (3) exhibits an ESR signal (X-band, toluene solution) at room temperature ($\langle g \rangle$ = 2.01, peak to peak separation = 2200 G), although hyperfine coupling to ^{181}Ta ($I = {}^7/_2$, 99.988% abundant) was not resolved. This behavior of compound 3 can be contrasted to that of d^3 TaCl$_2$(PMe$_3$)$_4$[28] and TaCl$_2$(dmpe)$_2$,[29] the ESR signals of which show well-resolved hyperfine structure under similar experimental conditions. Hyperfine coupling in 3 becomes apparent at low temperatures (frozen toluene solution, −196 °C), and a small g anisotropy is observed; overlapping g values complicate the spectrum, but $\langle g_{av} \rangle \approx 1.94$ and $\langle a \rangle_{Ta} \approx 220$ G. (η^6-C_6Et_6)Ta(DIPP)$_2$ is quite easily oxidized, as is evident from a cyclic voltammetry experiment. Scanning through an irreversible oxidation wave at $E_{p,a} = -0.58$ V vs Ag/AgCl (THF solution) gives rise to several irreversible, ill-defined electrochemical processes, most likely reflecting the instability of the resulting cation under the experimental conditions, perhaps including the reaction of this cation with unoxidized 3. This remarkably accessible oxidation can be compared to the value for the tantalum(III) compound (η^6-C_6Me_6)Ta(DIPP)$_2$Cl (2), which oxidizes at $E_{p,a} = +0.10$ V vs Ag/AgCl.[30] Accordingly, (η^6-C_6Et_6)Ta(DIPP)$_2$ can be oxidized with PCl$_5$ in Et$_2$O solution to afford the starting complex Ta(DIPP)$_2$Cl$_3$(OEt$_2$), along with C_6Et_6 in near-quantitative yields.

Paramagnetic (η^6-C_6Et_6)Ta(DIPP)$_2$ (3) is much more stable thermally than its diamagnetic tantalum(III) analogues.[14] Although they are exceedingly air and moisture sensitive, solutions of 3 remain intact for months when stored under N$_2$ at room temperature. We anticipated that 3 would be highly reactive toward one-electron oxidants; however, few reactions were discovered of any synthetic utility. The principal reaction pathway involved the labilization of the C_6Et_6 ring in reactions from which no tractable organometallic products were isolated. Examples include the reactions of 3 with 1 equiv of NO(g) and the photolysis of 3 with Me$_3$COOCMe$_3$. The attempted

Scheme I

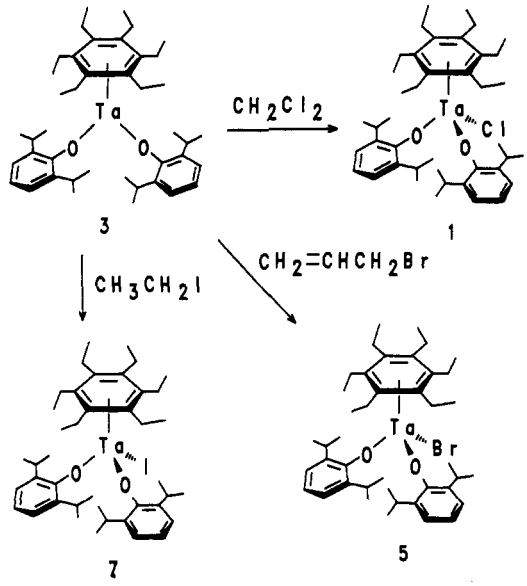

thermal reactions of 3 with *tert*-butyl peroxide gave no reaction.

Scheme I outlines the one-electron oxidative addition reaction of (η^6-C_6Et_6)Ta(DIPP)$_2$ (3) with alkyl and allyl halides to afford the tantalum(III) products (η^6-C_6Et_6)-Ta(DIPP)$_2$X (X = Cl, Br, I). An immediate reaction ensues between 3 and CH$_2$=CHCH$_2$Br to afford moderate yields of blue (η^6-C_6Et_6)Ta(DIPP)$_2$Br (5) (Scheme I). The same product is obtained upon reaction of 3 with other organic bromides, e.g. CH$_2$Br$_2$, BrCH$_2$CH$_2$Br, and CH$_3$CHBr$_2$, but in each of these cases, the product is contaminated with varying amounts of a diamagnetic green product. The reaction conditions can be manipulated to optimize the yield of this product. Thus, when 10 equiv of 1,2-dibromoethane is reacted with 3 for 15 min, a green, crystalline compound, which we formulate as the tantalum(III) dibromide complex (η^6-C_6Et_6)Ta(DIPP)Br$_2$ (6), is obtained in 32% yield, eq 3. It is likely that 6 arises

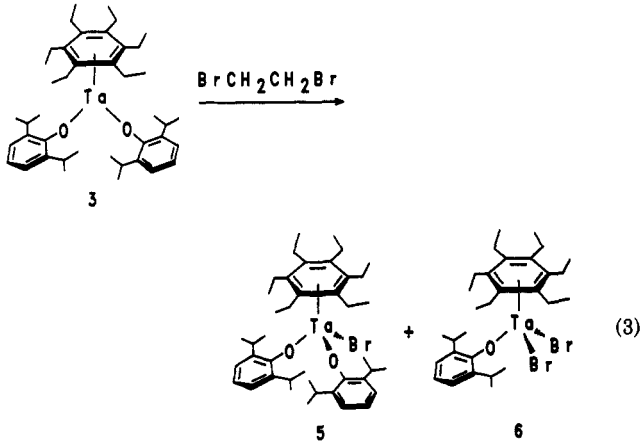

(3)

from the reaction of the kinetic product (η^6-C_6Et_6)Ta-(DIPP)$_2$Br (5) with excess 1,2-dibromoethane, since isolated 5 reacts with excess 1,2-dibromoethane to afford 6 and since solutions of pure 5 do not provide 6 upon their thermal decomposition.[31] These reactions are sufficiently

(28) (a) The original reports of this compound (refs 28b,c) suggested it was ESR silent, but it was later found to exhibit an eight-line ESR signal at $g = 1.93$ and $\langle a \rangle_{Ta} = 140$ G. See: Luetkens, M. L., Jr. Ph.D. Thesis, University of Michigan, 1984. (b) Luetkens, M. L., Jr.; Elcesser, W. L.; Huffman, J. C.; Sattelberger, A. P. *Inorg. Chem.* **1984**, *23*, 1718. (c) Luetkens, M. L., Jr.; Huffman, J. C.; Sattelberger, A. P. *J. Am. Chem. Soc.* **1983**, *105*, 4474.

(29) (a) Datta, S.; Wreford, S. S. *Inorg. Chem.* **1977**, *16*, 1134. (b) Luetkens, M. L., Jr.; Elcesser, W. L.; Huffman, J. C.; Sattelberger, A. P. *J. Chem. Soc., Chem. Commun.* **1983**, 1072.

(30) Strickler, J. R.; Bruck, M. A.; Wigley, D. E. *J. Am. Chem. Soc.* **1990**, *112*, 2814.

(31) We have reported a facile alkoxide–chloride exchange between (η^6-C_6Me_6)Ta(DIPP)$_2$Cl and Ta(DIPP)$_2$Cl$_3$(OEt$_2$) that affords high yields of the exchange products (η^6-C_6Me_6)Ta(DIPP)Cl$_2$ and Ta(DIPP)$_3$Cl$_2$-(OEt$_2$).[14] It was therefore deemed necessary to eliminate an alternate pathway for the formation of 6, viz. a similar methathesis reaction between two molecules of 5 to afford 6 and "(η^6-C_6Et_6)Ta(DIPP)$_3$".

Table II. Summary of Crystal Data and Data Collection Parameters for $(\eta^6\text{-}C_6Et_6)Ta(DIPP)_2$

mol formula	$C_{42}H_{64}TaO_2$
mol wt	781.92
space group	monoclinic, $P2_1/c$
unit cell volume, Å^3	3953.3
a, Å	12.396 (4)
b, Å	17.344 (6)
c, Å	18.622 (4)
β, deg	99.11 (2)
Z	4
calc den, g cm^{-3}	1.31
cryst dimen, mm	0.35 × 0.45 × 0.40
data collcn temp, °C	23 ● 1
λ(Mo Kα radiation), Å	0.71073
monochromator	graphite
abs coeff, cm^{-1}	27.8
transm coeff	0.882–0.998
2θ range, deg	2–50
total no. of reflns measd	7748 total, 7008 unique
no. of reflns measd with $I > 3\sigma(I)$	4581
scan type	θ–2θ
scan speed, deg min^{-1}	2–8
params refined	406
R	0.029
R_w	0.033

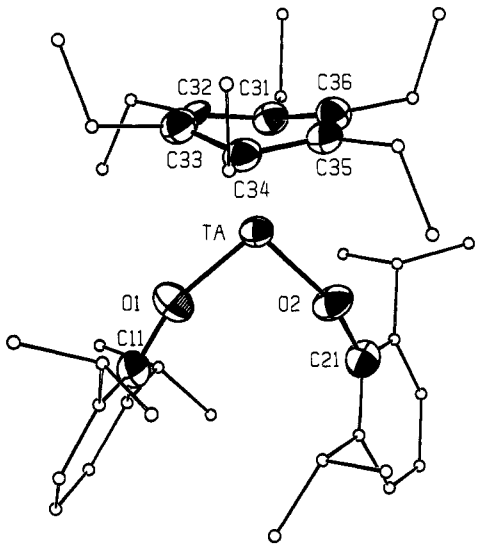

Figure 1. ORTEP drawing of $(\eta^6\text{-}C_6Et_6)Ta(DIPP)_2$ (DIPP = 2,6-diisopropyl phenoxide) with local coordination atoms shown as 50% ellipsoids.

complicated that we have not attempted to obtain any mechanistic information.

Structural Study of $(\eta^6\text{-}C_6Et_6)Ta(DIPP)_2$. $(\eta^6\text{-}C_6Me_6)Ta(DIPP)_2$ (4) did not provide crystals suitable for an X-ray structural determination; however, X-ray-quality crystals of $(\eta^6\text{-}C_6Et_6)Ta(DIPP)_2$ (3) were obtained from cold pentane solution. A summary of the crystal data and structural analysis is provided in Table II, positional parameters are given in Table III, and important bond distances and angles are listed in Table IV. Figure 1 presents an ORTEP drawing of $(\eta^6\text{-}C_6Et_6)Ta(DIPP)_2$, while Figure 2 presents a top view of the local coordination. The tantalum atom in this "two-legged piano stool" geometry is coordinated to two phenoxide ligands with Ta–O(1) = 1.917 (4) Å and Ta–O(2) = 1.916 (4) Å, and with Ta–O–C_{ipso} angles of 159.6 (4) and 158.2 (4)°, respectively. The most striking structural feature of 3 is the severe bending of the arene ligand, which results in C(31) and C(34) making close approaches to the metal (2.205 (5) and 2.219 (5) Å, respectively) while the remaining tantalum–carbon distances (average 2.386 Å) are more similar to those in known tantalum η^6-hexamethylbenzene complexes.[32]

Table III. Positional Parameters and Their Estimated Standard Deviations for $(\eta^6\text{-}C_6Et_6)Ta(DIPP)_2$[a]

atom	x	y	z	B, Å^2
Ta	0.21250 (2)	0.46254 (1)	0.25865 (1)	2.355 (3)
O(1)	0.2224 (3)	0.5254 (2)	0.1753 (2)	3.69 (8)
O(2)	0.3453 (3)	0.4982 (2)	0.3159 (2)	3.40 (8)
C(11)	0.2675 (5)	0.5658 (3)	0.1252 (3)	3.2 (1)
C(12)	0.2999 (5)	0.5267 (4)	0.0662 (3)	3.9 (1)
C(12A)	0.2806 (5)	0.4406 (4)	0.0554 (3)	4.3 (1)
C(12B)	0.3851 (8)	0.3960 (5)	0.0613 (6)	9.3 (3)
C(12C)	0.2059 (9)	0.4252 (6)	−0.0154 (5)	9.2 (3)
C(13)	0.3490 (6)	0.5697 (4)	0.0167 (4)	4.9 (2)
C(14)	0.3630 (6)	0.6470 (4)	0.0248 (4)	5.2 (2)
C(15)	0.3278 (6)	0.6850 (4)	0.0824 (4)	5.1 (2)
C(16A)	0.2427 (6)	0.6890 (4)	0.1952 (4)	5.1 (2)
C(16)	0.2800 (5)	0.6460 (3)	0.1337 (3)	4.0 (1)
C(16C)	0.3358 (7)	0.7313 (5)	0.2431 (4)	6.7 (2)
C(16B)	0.1489 (8)	0.7444 (5)	0.1667 (6)	8.6 (3)
C(21)	0.4257 (4)	0.5489 (3)	0.3437 (3)	3.1 (1)
C(22B)	0.5987 (7)	0.4405 (5)	0.2610 (5)	6.8 (2)
C(22)	0.5161 (5)	0.5578 (3)	0.3074 (3)	3.6 (1)
C(22A)	0.5278 (5)	0.5116 (4)	0.2404 (4)	4.1 (1)
C(22C)	0.5739 (7)	0.5594 (4)	0.1833 (4)	6.1 (2)
C(23)	0.5964 (5)	0.6094 (4)	0.3368 (4)	5.0 (2)
C(24)	0.5877 (6)	0.6508 (4)	0.3985 (4)	6.1 (2)
C(25)	0.4975 (6)	0.6417 (4)	0.4328 (4)	5.2 (2)
C(26A)	0.3180 (5)	0.5815 (3)	0.4451 (3)	3.8 (1)
C(26)	0.4152 (5)	0.5906 (3)	0.4068 (3)	3.6 (1)
C(26B)	0.2402 (6)	0.6497 (5)	0.4276 (5)	6.4 (2)
C(26C)	0.3492 (6)	0.5695 (5)	0.5263 (4)	6.1 (2)
C(31)	0.0763 (4)	0.4530 (3)	0.3213 (3)	2.8 (1)
C(32)	0.0224 (4)	0.4463 (3)	0.2445 (3)	2.7 (1)
C(33)	0.0567(4)	0.3895 (3)	0.1994 (3)	3.0 (1)
C(34)	0.1546 (4)	0.3452 (3)	0.2241 (3)	2.8 (1)
C(35)	0.1879 (4)	0.3385 (3)	0.3041 (3)	3.0 (1)
C(36)	0.1421 (4)	0.3874 (3)	0.3509 (3)	3.1 (1)
C(311)	0.0264 (5)	0.5081 (4)	0.3709 (3)	3.9 (1)
C(312)	−0.0752 (5)	0.4765 (5)	0.3989 (4)	5.8 (2)
C(321)	−0.0684 (5)	0.5027 (4)	0.2155 (4)	4.3 (1)
C(322)	−0.0297 (6)	0.5789 (4)	0.1881 (4)	5.1 (2)
C(331)	0.0046 (5)	0.3871 (4)	0.1202 (3)	4.5 (1)
C(332)	−0.1008 (7)	0.3398 (5)	0.1067 (5)	7.4 (2)
C(341)	0.1926 (5)	0.2829 (3)	0.1765 (3)	3.8 (1)
C(342)	0.1254 (6)	0.2080 (4)	0.1736 (4)	5.0 (2)
C(351)	0.2710 (5)	0.2772 (3)	0.3343 (4)	4.3 (1)
C(352)	0.3898 (6)	0.3016 (5)	0.3384 (5)	6.6 (2)
C(361)	0.1782 (5)	0.3799 (4)	0.4332 (3)	4.3 (1)
C(362)	0.1127 (7)	0.3171 (5)	0.4651 (4)	6.4 (2)

[a] Anisotropically refined atoms are given in the form of the isotropic equivalent displacement parameters defined as $(4/3)[a^2B(1,1) + b^2B(2,2) + c^2B(3,3) + ab(\cos\gamma)B(1,2) + ac(\cos\beta)B(1,3) + bc(\cos\alpha)B(2,3)]$.

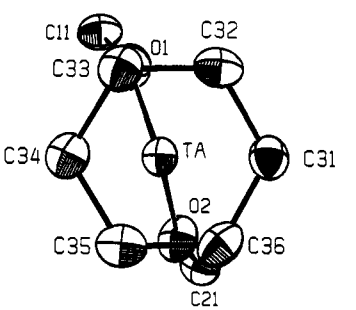

Figure 2. ORTEP drawing of the local coordination of $(\eta^6\text{-}C_6Et_6)Ta(DIPP)_2$ (DIPP = 2,6-diisopropyl phenoxide), viewed down the C_6Et_6(centroid)–Ta axis from an orientation perpendicular to the best arene plane. Atoms are shown as 50% ellipsoids.

Atoms C(31) and C(34) are well within the range of known Ta–C(sp^3) σ bonds of a metal–alkyl.[32] The extent of folding of the ring may be measured by the C(31)–C-

(32) Holloway, C. E.; Melnik, M. *J. Organomet. Chem.* **1986**, *303*, 39.

Table IV. Relevant Bond Distances (Å) and Angles (deg) for $(\eta^6\text{-}C_6Et_6)Ta(DIPP)_2$[a]

Bond Distances			
Ta–O(1)	1.917 (4)	O(1)–C(11)	1.355 (7)
Ta–O(2)	1.916 (4)	O(2)–C(21)	1.368 (6)
Ta–C(31)	2.205 (5)	C(31)–C(32)	1.486 (7)
Ta–C(32)	2.346 (5)	C(31)–C(36)	1.455 (8)
Ta–C(33)	2.424 (5)	C(32)–C(33)	1.403 (7)
Ta–C(34)	2.219 (5)	C(33)–C(34)	1.448 (7)
Ta–C(35)	2.349 (5)	C(34)–C(35)	1.486 (7)
Ta–C(36)	2.426 (5)	C(35)–C(36)	1.399 (8)
Bond Angles			
O(1)–Ta–O(2)	96.1 (2)	C(32)–C(33)–C(34)	120.1 (5)
O(1)–Ta–Arene[b]	129.7 (1)	C(33)–C(34)–C(35)	116.4 (5)
O(2)–Ta–Arene[b]	134.2 (1)	C(34)–C(35)–C(36)	120.1 (5)
Ta–O(1)–C(11)	159.6 (4)	C(35)–C(36)–C(31)	119.7 (5)
Ta–O(2)–C(21)	158.2 (4)	C(36)–C(31)–C(32)	116.3 (5)
C(31)–C(32)–C(33)	119.8 (5)		

[a] Numbers in parentheses are estimated standard deviations in the least significant digits. [b] "Arene" is the centroid of the C_6Et_6 ligand calculated by averaging the x, y, and z coordinates of all carbon atoms in the arene ring.

(32)–C(33)–C(34) plane, which assumes an angle of 20.8° out of planarity with C(34)–C(35)–C(36)–C(31). Arene bending to this extent is rare. (A compilation of folded arenes has been presented.[14]) Nonplanarity of this type (with two carbons closer to the metal) in η^6-arene ligands has also been observed in complexes of titanium,[10a] rhodium,[6a] ruthenium,[7b] and niobium,[33] but only in the case of related tantalum complexes $(\eta^6\text{-}C_6Me_6)Ta(DIPP)_2Cl$[12a] and $(\eta^6\text{-}C_6Me_6)Ta(DIPP)Cl_2$[14] is bending more severe than in **3** (fold angles 34.4 and 26.8°, respectively). Additionally, the arene ligand features considerable π electron localization as indicated by the short C(32)–C(33) and C(35)–C(36) bonds (1.403 (7) and 1.399 (8) Å, respectively), while the remaining carbon–carbon bond lengths range from 1.448 (7) to 1.486 (7) Å.

Two other structural features are noteworthy. First, the arene ring shows a distortion toward a twist-boat structure as C(33) and C(36) lie 0.05 Å above the least squares C(32)–C(33)–C(35)–C(36) plane, while C(32) and C(35) lie 0.05 Å below that plane. Secondly, as seen in Figure 2, the Ta–O–C_{ipso} linkages neither perfectly eclipse nor stagger the C–C bonds of the arene ring. To understand the bonding and structural features of **3**, we have undertaken a molecular orbital study of the model compound $(\eta^6\text{-}C_6H_6)Ta(OH)_2$, as described in the following section.

Computational Study of $(\eta^6\text{-}C_6H_6)Ta(OH)_2$. The electronic reasons that the arene ligand in 18-electron $(\eta^6\text{-arene})ML_2$ complexes distorts toward a nonplanar, boatlike geometry have been established.[34] Since the HOMO in this molecule is metal d centered, antibonding to a benzene π orbital, this antibonding is reduced when the arene distorts to a boat geometry. Consistent with this argument is the fact that upon removal of the electrons from the HOMO to give a 16-electron complex, the arene ring returns to planarity.[35] For the 13-electron, $(\eta^6\text{-arene})Ta(OR)_2$ molecules considered here, this orbital is also clearly not occupied. Therefore, we have turned to molecular orbital calculations at the extended Hückel and ab initio levels to discern the electronic driving force for the peculiar twist-boat deformation observed in $(\eta^6\text{-}C_6Et_6)Ta(DIPP)_2$ (**3**).

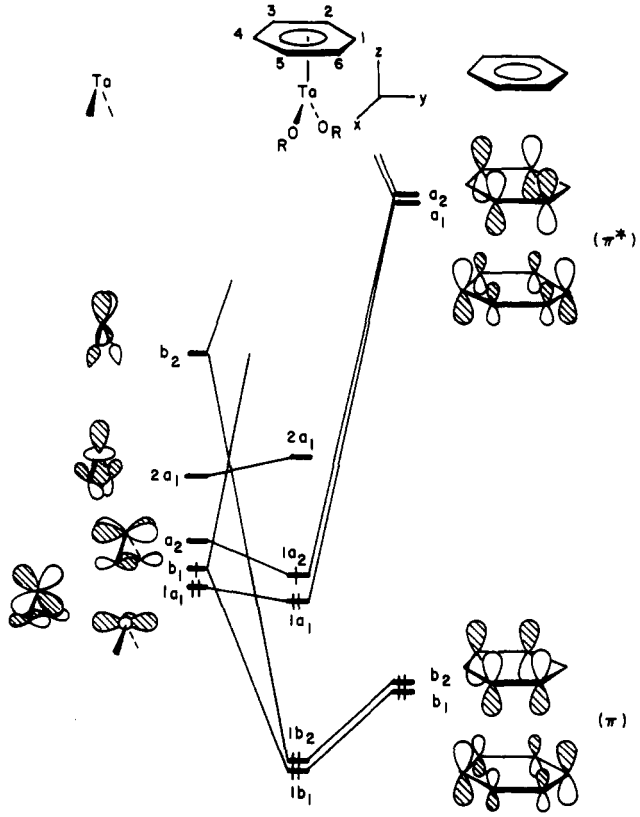

Figure 3. Orbital interaction diagram for $(\eta^6\text{-}C_6H_6)Ta(OR)_2$.

An idealized orbital interaction diagram for an $(\eta^6\text{-}C_6H_6)Ta(OR)_2$ molecule is given in Figure 3. Two of the benzene π and two π^* orbitals are shown on the right side of the figure. The fragment orbitals for an ML_2 unit, where L is a σ donor or has π acceptor functions, have been described elsewhere.[34,36] In this particular case, however, the alkoxide group possesses a σ donor orbital, **8**, as well

8 **9**

as two excellent π donor orbitals, **9**. The presence of the π donor functions requires some additional discussion. The highest lying fragment orbital, b_2, on the left side of Figure 3 is primarily xz antibonding to the alkoxide σ donor set. Furthermore, significant metal x character mixes into this orbital to hybridize it toward the benzene. At lower energies are the $2a_1$, a_2, and b_1 fragment levels. Each is primarily metal d in character, antibonding to the appropriate symmetry-adapted π donor set on the alkoxide ligands, as shown in Figure 3. The Ta–O–H angles were idealized at 180° for the extended Hückel (but not ab initio) calculations. As one can see in Figure 2, the Ta–O–C angles are in fact slightly bent to approximately 159°. The effect of this geometrical perturbation is quite minimal. The $2a_1$ orbital in Figure 3 is slightly stabilized. The lowest energy fragment orbital for $Ta(OR)_2$ is $1a_1$. This orbital is $x^2 - y^2$ and, most importantly to the ensuing discussion, contains metal s character. To see how this hybridization comes about, consider the interaction of the symmetric combination of two σ donor functions, **8**, on the alkoxides

(33) (a) Goldberg, S. Z.; Spivack, B.; Stanley, G.; Eisenberg, R.; Braitsch, D. M.; Miller, J. S.; Abkowitz, M. *J. Am. Chem. Soc.* **1977**, *99*, 110. (b) Churchill, M. R.; Chang, S. W.-Y. *J. Chem. Soc., Chem. Commun.* **1974**, 248. (c) Stollmaier, F.; Thewalt, U. *J. Organomet. Chem.* **1981**, *222*, 227.

(34) See ref 9a. (b) Albright, T. A.; Hoffmann, R.; Tse, Y.; D'Ottavio, T. *J. Am. Chem. Soc.* **1979**, *101*, 3812. (c) Chinn, J. W., Jr.; Hall, M. B. *J. Am. Chem. Soc.* **1983**, *105*, 4930.

(35) For a review of these structures, see ref 1b.

(36) Albright, T. A.; Burdett, J. K.; Whangbo, M.-H. *Orbital Interactions in Chemistry*; Wiley: New York, 1985.

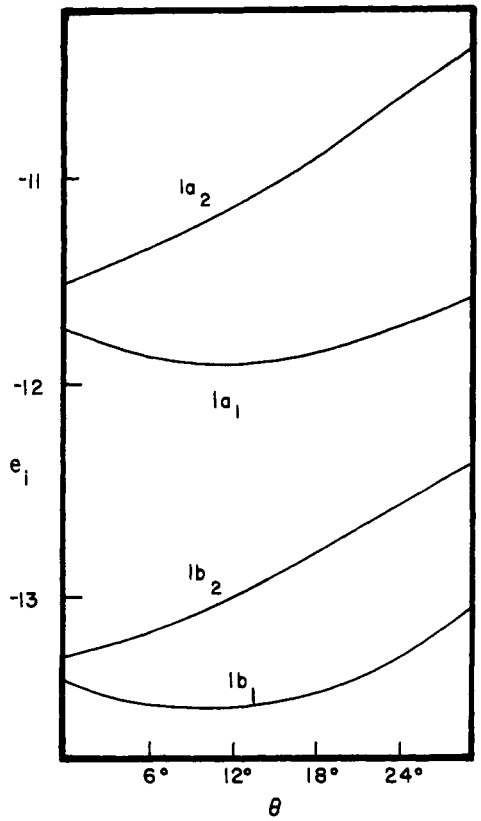

Figure 4. Plot of the orbital energy, e_i, for the four occupied molecular orbitals in Figure 3 versus θ, defined in **12** for $(\eta^6\text{-}C_6H_6)Ta(OH)_2$.

with the $x^2 - y^2$ and s atomic orbitals on Ta. A typical[36] three-orbital pattern results, as shown in **10**. The σ donor

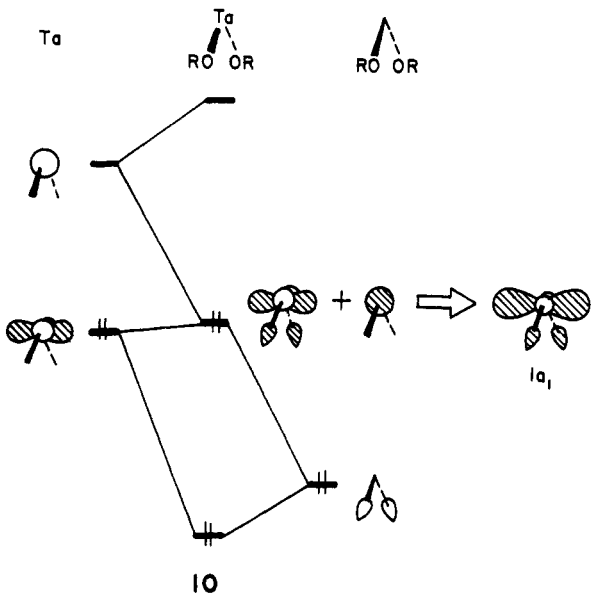

10

set is stabilized by $x^2 - y^2$ and s. The middle level, which corresponds to the $1a_1$ fragment orbital, is primarily $x^2 - y^2$ with some σ donor character mixed in an antibonding way. However, metal s also mixes into the orbital in second order[36] with the phase shown. This serves to reduce the metal–alkoxide antibonding and consequently $1a_1$ remains at a low energy and is a nonbonding orbital. What is central to our discussion of arene bending is the fact that the $x^2 - y^2/s$ hybridization in $1a_1$ reduces the amplitude of this fragment orbital in the $Ta(OR)_2$ plane and increases the amplitude in the plane orthogonal to it.

Table V. Geometrical Parameters and Relative Energies for $(\eta^6\text{-}C_6H_6)Ta(OH)_2$ at the ab Initio Level

variable	11	12	14	15	18	expt[a]
Ta–C_1, Å	2.47	2.33	2.43	2.50	2.21	2.212 (5)
Ta–C_2, Å	2.47	2.50	2.43	2.44	2.58	2.348 (5)
Ta–C_3, Å	2.47	2.50	2.43	2.44	2.60	2.425 (5)
C_1–C_2, Å	1.42	1.44	1.42	1.43	1.50	1.486 (7)
C_2–C_3, Å	1.42	1.39	1.42	1.40	1.35	1.401 (8)
C_3–C_4, Å	1.42	1.44	1.42	1.43	1.49	1.452 (8)
Ta–O, Å	1.87	1.90	1.89	1.87	1.89	1.917 (4)
O–Ta–O, deg	105.0	98.1	100.5	106.2	104.1	96.1 (2)
Ta–O–R, deg	177.1	169.8	177.3	177.2	165.9	158.9
ϕ,[b] deg	0.0	0.0	90.0	90.0	27.2	15.6
rel energy, kcal/mol	19.8	13.9	18.2	15.9	0.0[c]	

[a] The experimental values for compound **3** in this study. Averaged values are reported. [b] The rotation angle about the benzene–Ta axis, as defined in **17**. [c] The absolute energy was -436.80060 au.

Returning to Figure 3, the two benzene π orbitals are stabilized by the b_2 and b_1 fragment orbitals on $Ta(OR)_2$. The $1a_1$ and a_2 fragment orbitals have δ symmetry with respect to the benzene. They are, therefore, stabilized by the benzene π^* set. Finally, the $Ta(OR)_2$ $2a_1$ orbital remains essentially nonbonding. Notice that the $1a_1$ molecular orbital lies lower in energy than $1a_2$. This level ordering is ensured because $1a_1$ is nonbonding but a_2 is clearly antibonding to the alkoxide ligand set. Consequently, molecular $1a_1$ is filled and $1a_2$ is singly occupied for this d^3 complex.

Let us now consider the changes which occur for the occupied molecular orbitals in Figure 3 when the planar benzene ligand is distorted to a boat geometry. A Walsh diagram based upon extended Hückel calculations for going from **11** to **12** is shown in Figure 4. Here θ is defined

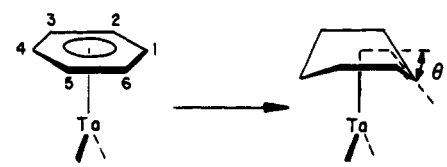

11 **12**

as the angle made between the C(2)–C(1)–C(6) and C(3)–C(4)–C(5) planes with the C(2)–C(3)–C(5)–C(6) plane. The molecular $1b_2$ and $1a_2$ orbitals rise in energy as θ increases. The reason for this is rather simple. As θ increases, the z atomic orbitals on C(2), C(3), C(5), and C(6) reorient themselves, as shown in a somewhat exaggerated manner in **13**. Overlap between the b_2 and a_2 fragment

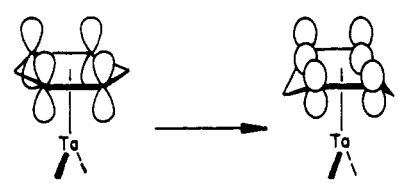

13

orbitals (Figure 3) on $Ta(OH)_2$ and the appropriate π and π^* orbitals on the benzene is reduced. For example, the overlap of b_2 with π, $\langle b_2|\pi\rangle$, at $\theta = 0°$ is 0.328 while that at $\theta = 24°$ is 0.238. The corresponding values for $\langle a_2|\pi^*\rangle$ at $\theta = 0°$ and $\theta = 24°$ are 0.139 and 0.110, respectively. On the other hand, the molecular $1b_1$ and $1a_1$ orbitals initially are stabilized as θ increases. Here there is increased overlap between the atomic z orbitals at C(1) and C(4) with the $1a_1$ and b_1 fragment orbitals on $Ta(OH)_2$. For example, $\langle b_1|\pi\rangle = 0.233$ and 0.287 at $\theta = 0$ and 30°, respectively, and $\langle 1a_1|\pi^*\rangle$ increases from 0.073 to 0.146 for these two angles.

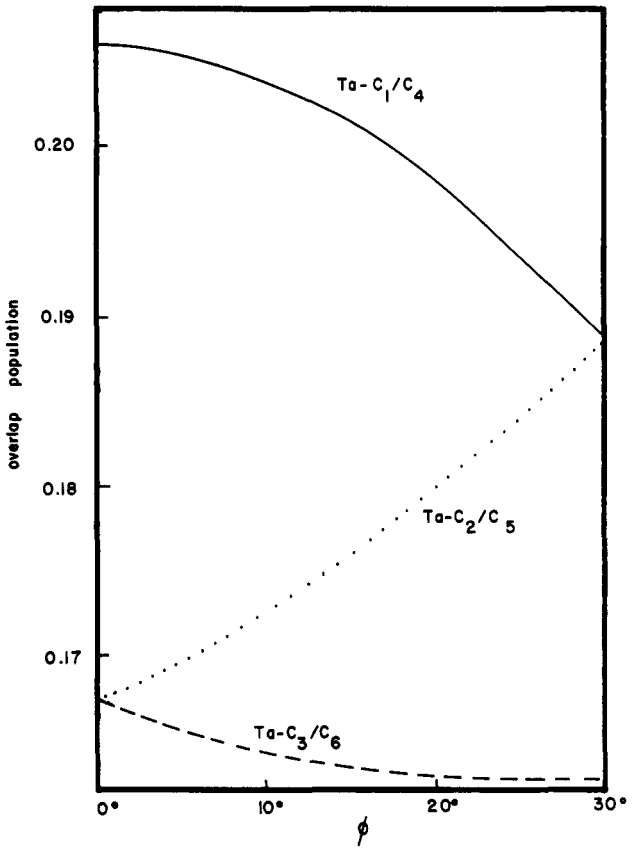

Figure 5. Ta–C overlap populations versus the rotational angle, ϕ, defined in 17 for $(\eta^6\text{-}C_6H_6)Ta(OH)_2$.

At large values of θ, lower lying σ levels on the benzene skeleton also begin to mix into the molecular $1b_1$ and $1a_1$ orbitals, which causes them to be destabilized. At small to intermediate values of θ, the energetic behaviors of $1b_1$ and $1b_2$ approximately cancel one another. The same would be true for the $1a_2$ and $1a_1$ levels; however, $1a_1$ is doubly occupied whereas $1a_2$ is occupied with a single electron. Therefore, the distortion from 11 to 12 results in a net stabilization. At the ab initio level all internal coordinates were optimized within a C_{2v} symmetry constraint, except that in structure 11 the benzene ring was also forced to remain planar with equal C–C and C–H bond lengths. Relevant geometrical parameters are listed in Table V. It was found that 12 is 5.9 kcal/mol more stable than 11 with an optimized value of $\theta = 17.9°$.

Structure 12 is certainly not the only viable conformation for $(\eta^6$-arene$)Ta(OR)_2$ complexes. Rotation about the benzene–Ta axis by 90° (or the equivalent 30° rotation) produces 14. Returning to Figure 3, rotation of the Ta-

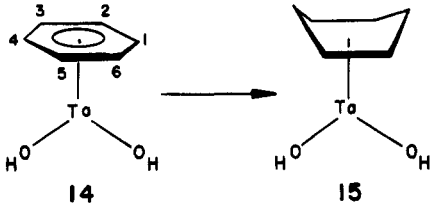

14 15

$(OR)_2$ unit by 90° simply interchanges the b_1 and b_2 symmetry labels for that moiety. Since the benzene π set is degenerate, the energy difference between conformations 11 and 14 is expected to be quite small. Indeed, at the ab initio level, we find that the energy of optimized 14 (see Table V) is 1.6 kcal/mol lower than that in 11. Again there is a sizable potential for deformation to a boat conformation given by 15. The controlling factor is again the energetic behavior of the $1a_1$ molecular orbital. A bottom view of this molecular orbital is given in 16. With the

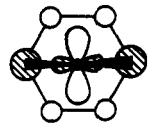

16

hybridization in the $1a_1$ fragment orbital on $Ta(OR)_2$, there is now stronger bonding to C(2), C(3), C(5), and C(6). Consequently, the folding of these carbon atoms downward, toward Ta serves to further stabilize molecular $1a_1$. Notice that the rotational difference of the $Ta(OH)_2$ unit in 12 and 15 directly results in different boatlike deformations of the benzene ligand. At the ab initio level, the fully optimized geometry of 15 (see Table V) lies 2.3 kcal/mol lower in energy than that of 14. The folding angle of C(1) and C(4) (defined in an analogous way to that shown in 12) is 8.3°.

The full itinerary for rotation about the benzene–Ta axis can then be regarded as a superposition of the effects in conformations 12 and 15. Let ϕ be this rotational angle, defined by 17. When $\phi = 0°$ (12′), C(1) and C(4) move

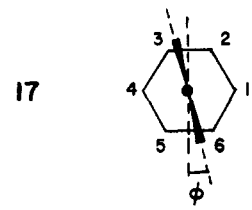

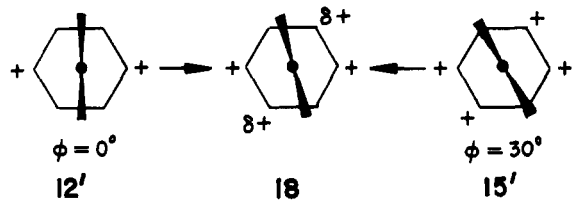

12′ 18 15′

toward the Ta, and at $\phi = 30°$ (15′), C(1), C(2), C(4), and C(5) move in this direction. Therefore, at an intermediate geometry, 18, C(1) and C(4) are most strongly distorted toward Ta followed by C(2) and C(5) to a lesser extent. A way to show this situation in a more quantitative fashion is given in Figure 5. Here the Ta–C overlap population is plotted as a function of the rotational angle, ϕ, for $(\eta^6\text{-}C_6H_6)Ta(OH)_2$ at the extended Hückel level; all Ta–C distances are kept equal and constant along the rotational path. For any intermediate value of ϕ the overlap populations are always in the order Ta–C(1)[C(4)] > Ta–C(2)[C(5)] > Ta–C(3)[C(6)]. A larger Ta–C overlap population implies that the bond distance should become shorter; hence, the Ta–C distances should order themselves as Ta–C(1)[C(4)] < Ta–C(2)[C(5)] < Ta–C(3)[C(6)]. This is exactly the experimental sequence found in 3. At an intermediate value of ϕ, the symmetry is reduced from C_{2v} to C_2. The molecular orbitals $1a_1$ and $1a_2$ (Figure 3) both have a symmetry, so they will intermix. This stabilizes the former and destabilizes the latter. The resultant situation will be stabilizing, since $1a_2$ is only singly occupied. A full optimization with C_2 symmetry constraints at the ab initio level for 18 clearly shows these patterns (Table V). The agreement between experiment and theory is satisfactory except for two features. Firstly, the Ta–C(2) and Ta–C(3) bond lengths are computed to be considerably longer than the experimental ones. This is reminiscent of the typical situation for metal–carbon bond lengths in polyene–metal complexes at the Hartree–Fock level.[37] We

suspect that inclusion of some electron correlation will dramatically improve the results, as it has been documented for the other situations.[37] Secondly, the optimized value of the Ta–benzene rotation angle, ϕ, is certainly too large. However, the potential energy surface around the optimized C_2 geometry was found to be extremely flat. In fact a single point calculation with ϕ set at the experimental value (15.6°) and fixing *all* other internal coordinates to their optimized values in 18 resulted in an energy expenditure of only 2.1 kcal/mol. Notice that the pattern of a short C(2)–C(3) (and C(5)–C(6)) distance compared to the others in 3 and reproduced in 18 is a direct result of the larger occupation of the a_1 π^* orbital on benzene compared to a_2 (see Figure 3). The a_1 orbital is bonding between C(2) and C(3), while it is antibonding between C(1)–C(2) and C(3)–C(4).

The peculiar twist-boat conformation in 3 is, therefore, tied to the hybridization presented in the $x^2 - y^2$ orbital on Ta along with the fact that the $1a_1$ molecular orbital in Figure 3 is doubly occupied, whereas $1a_2$ is occupied with a single electron. The substantial buckling of the arene ring and its C–C bond localization underscore the fact that there is extremely strong δ-type bonding between the arene and Ta in these complexes compared to the situation that exists for other 16–18-electron (η^6-arene)ML_n systems.[34,35] The addition of another electron to $1a_2$ should then cause the arene to return to planarity and greatly reduce the rotational barrier around the arene–Ta axis. A one-electron reduction of 3 is not particularly facile, as seen in its electrochemical reduction, which occurs at ca. −1.7 V vs Ag/AgCl. The reason for this is that strong π bonding exists between the alkoxide oxygen atoms and Ta. This is evidenced in the structure of 3 and the model calculations since the Ta–O–R angle (see Table V) is extremely large. Therefore, a 14-electron (η^6-arene)TaL_2 candidate is more feasible with a weaker π donor set on the auxiliary ligands. We shall explore work along these lines in the future.

Acknowledgment. T.A.A. thanks the Robert A. Welch Foundation and the donors of the Petroleum Research Fund, administered by the American Chemical Society, for support and the NSF for a generous allocation of computer time to the Pittsburgh Supercomputing Center. D.E.W. thanks the NSF (Grant CHE-8919367) for support of this work and the donors of the Petroleum Research Fund, administered by the American Chemical Society, for partial support.

Supplementary Material Available: Textual presentation of data collection and reduction and structure solution and refinement, tables of the structure solution and crystallographic details for (η^6-C_6Et_6)$Ta(DIPP)_2$, atomic positional and thermal parameters, bond distances and angles, least-squares planes, dihedral angles, and ORTEP figures and full listings of the internal coordinates and total energies for (η^6-C_6H_6)$Ta(OH)_2$ (26 pages); tables of observed and calculated structure factor amplitudes (20 pages). Ordering information is given on any current masthead page.

(37) (a) Williamson, R. L.; Hall, M. B. *Int. J. Quantum Chem., Quantum. Chem. Symp.* **1987**, *21*, 503. (b) Taylor, T. E.; Hall, M. B. *Chem. Phys. Lett.* **1985**, *114*, 338. (c) Lüthi, H. P.; Siegbahn, P. E. M.; Almlöf, J.; Faegri, K., Jr.; Heiberg, A. *Ibid.* **1984**, *111*, 1. (d) Kang, S.-K.; Albright, T. A. Unpublished calculations.

Reactions of the Neohexyl Iodide Complex $[(\eta^5\text{-}C_5H_5)Re(NO)(PPh_3)(ICH_2CH_2C(CH_3)_3)]^+BF_4^-$ and Nucleophiles: Stereochemistry of Carbon–Iodine Bond Cleavage in Highly Accelerated S_N2 Reactions

Alain Igau and J. A. Gladysz*

Department of Chemistry, University of Utah, Salt Lake City, Utah 84112

Received January 3, 1991

Reaction of (η^5-C_5H_5)Re(NO)(PPh_3)(CH_3), $ICH_2CH_2C(CH_3)_3$ (2), and HBF_4·OEt_2 in C_6H_5Cl gives neohexyl iodide complex $[(\eta^5\text{-}C_5H_5)Re(NO)(PPh_3)(ICH_2CH_2C(CH_3)_3)]^+BF_4^-$ (3, 81%). Complex 3 and PPh_3 react (−40 °C, CD_2Cl_2) to give $[Ph_3PCH_2CH_2C(CH_3)_3]^+BF_4^-$ (7) and (η^5-C_5H_5)Re(NO)(PPh_3)(I) (6) in >99% spectroscopic yields. Complex 3 and $[Ph_3P{=}N{=}PPh_3]^+Br^-$ (PPN^+Br^-) react (−40 °C, CD_2Cl_2) to give $BrCH_2CH_2C(CH_3)_3$ (8) and 6 in 97–99% spectroscopic yields. Deuterated neohexyl halides *erythro*-$ICHDCHDC(CH_3)_3$ (*erythro*-2-d_2), *threo*-2-d_2, *erythro*-8-d_2, and *threo*-8-d_2 are prepared via (η^5-$C_5H_5)_2Zr(Cl)(X)$ compounds. The labeled complexes *erythro*-3-d_2 and *threo*-3-d_2 are synthesized, and analogous reactions with PPN^+Br^- and PPh_3 are conducted. Diastereomer ratios of the products 8-d_2 and 7-d_2, and all preceding deuterated compounds, are analyzed by 500-MHz $^1H\{^2H\}$ NMR spectroscopy. In all cases, the carbon–iodine bond in 3-d_2 is cleaved with essentially complete *inversion* of configuration at carbon.

Ten years ago, stable transition-metal complexes of alkyl halides were unknown. Since the pioneering 1982 study by Crabtree, the isolation of a variety of alkyl halide complexes has been reported.[1-7] Accordingly, there has been a surge of interest in the coordination chemistry of alkyl halide ligands.

(1) Kulawiec, R. J.; Crabtree, R. H. *Coord. Chem. Rev.* **1990**, *99*, 89.

(2) (a) Crabtree, R. H.; Faller, J. W.; Mellea, M. F.; Quirk, J. M. *Organometallics* **1982**, *1*, 1361. (b) Burk, M. J.; Segmuller, B.; Crabtree, R. H. *Ibid.* **1987**, *6*, 2241. (c) Kulawiec, R. J.; Faller, J. W.; Crabtree, R. H. *Ibid.* **1990**, *9*, 745 and references therein.

0276-7333/91/2310-2327$02.50/0